Study of the Structural Modifications Induced by Reducing Treatments on a Pd/$Ce_{0.8}Tb_{0.2}O_{2-x}$/La_2O_3−Al_2O_3 Catalyst by Means of X-ray Diffraction and Electron Microscopy Techniques

S. Bernal,[†] J. J. Calvino,[†] G. A. Cifredo,[†] D. Finol,[†] J. M. Gatica,[†] C. J. Kiely,[‡]
C. López-Cartes,[†] J. G. Zheng,[‡] and H. Vidal*,[†]

Departamento de Ciencia de los Materiales e Ingeniería Metalúrgica y Química Inorgánica, Facultad de Ciencias, Universidad de Cádiz, Apartado 40, 11510 Puerto Real (Cádiz), Spain, and Departments of Chemistry and Engineering, University of Liverpool, L69 3BX U.K.

Received October 18, 2001. Revised Manuscript Received November 19, 2001

X-ray diffraction with Rietveld analysis, EDS, HREM, and CO oxidation experiments have been used to study the nanoscale evolution with reduction temperature of a Pd/$Ce_{0.8}Tb_{0.2}O_{2-x}$/La_2O_3−Al_2O_3 catalyst. Up to 700 °C, both Pd and the $Ce_{0.8}Tb_{0.2}O_{2-x}$ mixed oxide are present as nanosized particles that are well-dispersed over the La-modified alumina support. After reduction at 900 °C, severe sintering of the metallic Pd particles occurs, along with the formation of a perovkite phase $LnAlO_3$ with variable content of trivalent lanthanide ions ($Ln^{3+} = La^{3+}$, Ce^{3+}, and Tb^{3+}). Parallel deactivation of the catalyst for the CO oxidation reaction is observed upon increasing reduction temperature.

1. Introduction

Metal/ceria/alumina systems have acquired a great relevance in the formulation of three-way catalysts.[1] Selection of Pd, in particular, as the metallic phase is well-known to be an interesting alternative compared to Rh and Pt,[2,3] also because of its outstanding behavior for light-hydrocarbon combustion reactions, especially those involving methane.[4] Likewise, as recently reported in refs 5 and 6, the incorporation of terbium as a promoter allows for an improvement of the redox performance of M/CeO_2-based catalysts. In a previous paper,[7] we reported on the structural and chemisorption properties of a Ce/Tb mixed oxide dispersed on a lanthana-modified alumina, paying special attention to its thermal stability under different environments. This study showed that the supported cerium/terbium oxide resisted degradation at 700 °C under reducing conditions. The modification of the alumina surface with lanthana seems to block the interaction of the Ce/Tb lanthanide ions with the alumina support. On this basis, the above system was shown to be a potential support of metal phases for TWC applications.

Resistance against deactivation phenomena is currently recognized as one of the major targets in TWC technology.[8] As these systems operate in real working conditions under continuously cycling reducing and oxidizing environments at high temperature,[9] determining in detail how their structure changes as a consequence of high-temperature oxidation and reduction treatments becomes of obvious interest. Therefore, in this work, we have focused on the nanostructural evolution undergone by a Pd/$Ce_{0.8}Tb_{0.2}O_{2-x}$/La_2O_3−Al_2O_3 sample when subjected to reducing treatments over a wide range of reduction temperatures. Such studies can help to elucidate the processes responsible for the deactivation of these catalysts. For this purpose, a series of samples treated under reducing environments of increasing severity has been characterized using a battery of complementary techniques including X-ray diffraction (XRD) with Rietveld analysis, high-resolution electron microscopy (HREM), and energy dispersive spectroscopy (EDS). Additional experiments were performed to evaluate the catalytic behavior in the oxidation of CO, one of the reactions of interest in the TWC process. To our knowledge, no such results on a Pd/$Ce_{0.8}Tb_{0.2}O_{2-x}$/La_2O_3−Al_2O_3 catalyst have been published prior to this research.

2. Experimental Section

2.1. Sample Preparation. The 16% $Ce_{0.8}Tb_{0.2}O_{2-x}$/13% La_2O_3−Al_2O_3 oxide used as a support in this work was

---

* To whom correspondence should be addressed. Phone: 34-956-016334. Fax: 34-956-016288. E-mail: hilario.vidal@uca.es.

[†] Universidad de Cádiz.

[‡] University of Liverpool.

(1) Trovarelli, A. *Catal. Rev. Sci. Eng.* **1996**, *38* (4), 439.

(2) Jen, H. W.; Graham, G. W.; Chun, W.; McCabe, R. W.; Cuif, J. P.; Deutsch, S. E.; Touret, O. *Catal. Today* **1999**, *50*, 309.

(3) Van Yperen, R.; Lindner, D.; Muβmann, L.; Lox, E. S.; Kreuzer, T. *Stud. Surf. Sci. Catal.* **1998**, *116*, 51.

(4) Farrauto, R. J.; Hobson, M. C.; Kennelly, T.; Waterman, E. M. *Appl. Catal. A: Gen.* **1992**, *81*, 227.

(5) Bernal, S.; Blanco, G.; Cauqui, M. A.; Corchado, P.; Pintado, J. M.; Rodríguez-Izquierdo, J. M.; Vidal, H. *Stud. Surf. Sci. Catal.* **1998**, *116*, 611.

(6) Bernal, S.; Blanco, G.; Cauqui, M. A.; Corchado, P.; Pintado, J. M.; Rodríguez-Izquierdo, J. M. *Chem. Commun.* **1997**, 1545.

(7) Bernal, S.; Blanco, G.; Cifredo, G. A.; Finol, D.; Gatica, J. M.; Rodríguez-Izquierdo, J. M.; Vidal, H. *Chem. Mater.*, in press.

(8) Degobert, P. *Automobiles and Pollution*; Society of Automotive Engineers, Inc.: Warrendale, PA, 1995.

(9) Hech, R. M.; Farrauto, R. J. *CATTECH* **1997**, *2*, 197.

10.1021/cm011260y CCC: $22.00

prepared following the method reported in ref 7. The Pd-containing sample was obtained by impregnating this support to incipient wetness in three cycles. A $[Pd(NH_3)_4](NO_3)_2$ solution with pH = 9 was employed as the metal precursor to avoid the support leaching effects that are known to occur under acidic conditions.[10] The concentration of the impregnating solution was adjusted so as to introduce a metal loading of 7% (referred to each gram of support). After impregnation, the sample was dried at 80 °C and further calcined in air at 500 °C for 2 h, before being stored in the oxidized state until time of use.

After the preparation and prior to the catalytic assays, the sample was submitted to an "in situ" cleaning pretreatment consisting of being heated in a flow of O_2 (5%)/He for 1 h at 550 °C and then cooled under a flowing O_2 (5%)/He mixture down to 150 °C and, finally, in a flow of He to room temperature. With this protocol, a reproducible starting redox state for the supported Ce/Tb mixed oxide can be obtained.[11]

The reduction treatments consisted of heating the sample under flowing H_2 (5%)/Ar (60 $mL \cdot min^{-1}$) from 25 °C to the selected reduction temperature (T_{redn}) at a rate of 10 $°C \cdot min^{-1}$. The sample was kept at T_{redn} for 1 h, then the gas flow was switched to Ar (60 $mL \cdot min^{-1}$) for 1 h, and finally, the sample was cooled to room temperature, always under flowing Ar.

To avoid rapid uncontrolled reoxidation of the reduced samples upon exposure to air, the samples were submitted to a passivation protocol at low temperature, consisting of the following steps: (1) cooling to −80 °C (solid/liquid acetone trap) in a flow of inert gas; (2) treatment with an O_2 (5%)/He mixture at −80 °C for 1 h, and finally, (3) free warming to room temperature in the mild oxidizing mixture.[12] After this treatment, the sample was exposed to air and characterized by XRD and TEM.

2.2. Characterization Techniques. X-ray diffraction was performed at room temperature using a powder Philips PW1820 diffractometer, operating with Cu Kα radiation. The 2θ angle ranged from 10 to 130°, and the counting step interval was 0.02°. In the case of the sample calcined at 500 °C, i.e., prior to any reduction treatment, Rietveld analysis of the experimental diffractogram was performed using the program Fullprof.[13]

The HREM images shown in this work were recorded on a JEOL 2000 EX microscope equipped with a top-entry specimen holder, its point-to-point resolution being 0.21 nm. The structural models employed as supercells for image calculations were built using the RHODIUS program,[14] and simulated HREM images were obtained using EMS.[15] Digital diffractograms (DDPs) were calculated using SEMPER 6+ software. The EDS spectra were obtained in a VG HB601 scanning transmission electron microscope operating at 100 kV using a 1-nm probe. X-ray acquisition was carried out on an Oxford ex12 EDS system having a windowless Si(Li) detector.

Finally, for the carbon monoxide oxidation reaction studies, CO (5%)/He and O_2 (5%)/He mixed in a stoichiometric ratio were used, the total gas flow being 60 $mL \cdot min^{-1}$. On-line analysis of the products was carried out using a Spectralab SX 200 mass spectrometer. CO conversion was monitored by using the MS signal for CO (*m/e* 28) after subtraction of the contribution from CO_2 formation (*m/e* 44). The reaction was followed from room temperature to 900 °C at a heating rate of 10 $°C \cdot min^{-1}$. The light-off temperature was selected to correspond to a CO conversion of 50%.

3. Results and Discussion

3.1. X-ray Diffraction. Figure 1 shows the X-ray diffractogram recorded for the Pd-supported sample calcined in air at 500 °C for 2 h (S_{BET} = 92 m^2/g). For comparison purposes, the diagram corresponding to the support $Ce_{0.8}Tb_{0.2}O_{2-x}/La_2O_3-Al_2O_3$ is also included.

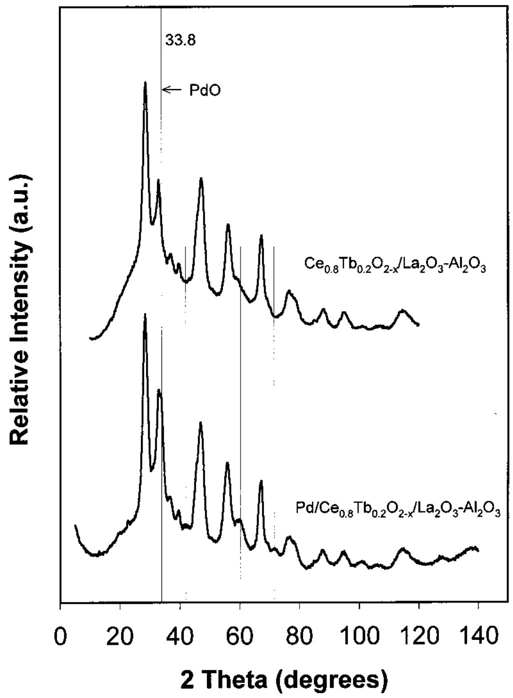

Figure 1. X-ray diffractogram obtained for the $Pd/Ce_{0.8}Tb_{0.2}O_{2-x}/La_2O_3-Al_2O_3$ catalyst calcined in air for 2 h at 500 °C. For reference, the spectrum obtained for the $Ce_{0.8}Tb_{0.2}O_{2-x}/La_2O_3-Al_2O_3$ support calcined in air 4 h at 700 °C has also been included. The diffraction line at 33.8° corresponds to tetragonal PdO.

According to Figure 1, the diffractogram of the Pd catalyst shows all of the peaks characteristic of the support, i.e., those attributed to the fluorite structure of the Ce/Tb supported mixed oxide and those due to the transition alumina used. In addition, a series of low-intensity peaks is observed that, although poorly resolved, can be assigned to tetragonal PdO [JCPDS 46-1224].

A more detailed interpretation of this diagram was carried out by Rietveld analysis (Rwp = 5.81 as defined in ref 13). As a result, the experimental spectrum was decomposed into six contributions (Figure 2) from the following phases: a fluorite-type mixed oxide of Ce/Tb (8.1%); θ-Al_2O_3 (48.4%); η-Al_2O_3 (35.1%); tetragonal PdO (space group *P*4*n*2) (5.7%); cubic palladium oxide with Pd_7O_8 stoichiometry (0.9%); and a perovskite, $LnAlO_3$ (1.8%). Therefore, in addition to confirming the phase identity, this analysis estimates the weight percentage of each phase present. The identification of other minority phases that were not detected by the mere observation of the diffractogram has also been achieved. Concerning these minority phases, we should highlight the sparse formation of perovskite, presumably by reaction of a small fraction of the dispersed lanthanum with the alumina support.[7] Likewise, it should be mentioned that the possibility of formation of other palladium oxides in addition to PdO under an oxidizing environment in supported palladium catalysts has been already reported in the literature.[16] No evidence of

---

(10) Bernal, S.; Blanco, G.; Cifredo, G. A.; Finol, D.; Gatica, J. M.; Vidal, H., manuscript in preparation.

(11) Eyring, L. *J. Solid State Chem.* **1970**, *1*, 376.

(12) Bernal, S.; Botana, F. J.; Calvino, J. J.; Cifredo, G. A.; Pérez-Omil, J. A.; Pintado, J. M. *Catal. Today* **1995**, *23*, 219.

(13) Rodríguez-Carvajal, J. J. *Physica B* **1993**, *192*, 55.

(14) Botana, F. J.; Calvino, J. J.; Blanco, G.; Marcos, M.; Pérez-Omil, J. A. *Electron Microsc.* **1994**, *2B*, 1085.

(15) Stadelmann, P. *Ultramicroscopy* **1987**, *21*, 197.

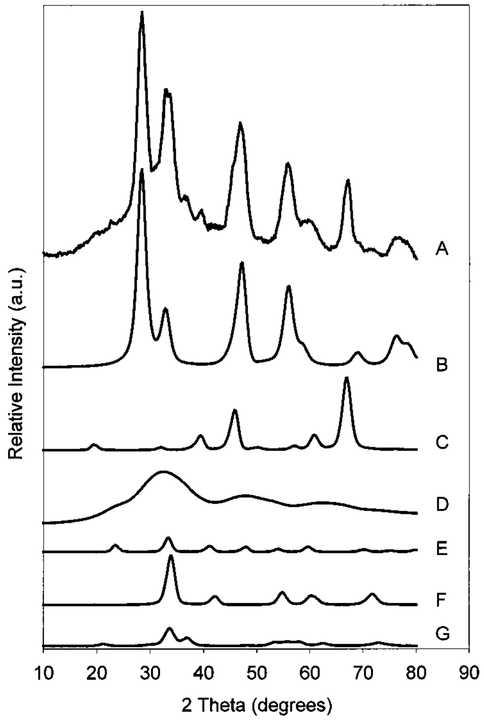

Figure 2. X-ray spectrum obtained for (A) the Pd/$Ce_{0.8}Tb_{0.2}O_{2-x}$/La_2O_3–Al_2O_3 catalyst calcined in air at 500 °C for 2 h and the phases present as deduced from Rietveld analysis: (B) $Ce_{0.8}Tb_{0.2}O_{2-x}$, (C) η-Al_2O_3, (D) θ-Al_2O_3, (E) $LnAlO_3$, (F) tetragonal PdO, and (G) cubic Pd_7O_8.

crystalline lanthanum-containing phases other than the minority perovskite could be obtained from this analysis.

Figure 3 shows the XRD spectra obtained for the Pd/$Ce_{0.8}Tb_{0.2}O_{2-x}$/La_2O_3–Al_2O_3 catalyst reduced at different temperatures. As a reference, the diffractogram recorded for the initial calcined sample is also included. A direct comparison of the different diffractograms reveals that the catalyst undergoes significant structural changes as the reduction temperature increases.

When the traces corresponding to the sample just calcined and that reduced at 350 °C are compared, some interesting differences can be discerned. First, although no significant changes are observed regarding the reflections characteristic of the promoter and the support, the peaks assigned to PdO in the calcined sample disappear in the diagram of the reduced catalyst. At the same time, relatively narrow and intense peaks at the position characteristic of metallic palladium are clearly observed, especially the one centered at $2\theta = 40.1°$, which corresponds to the most intense [111]-type diffraction maximum of the metallic fcc structure [JCPDS 46-1043]. These peaks have been marked in Figure 3.

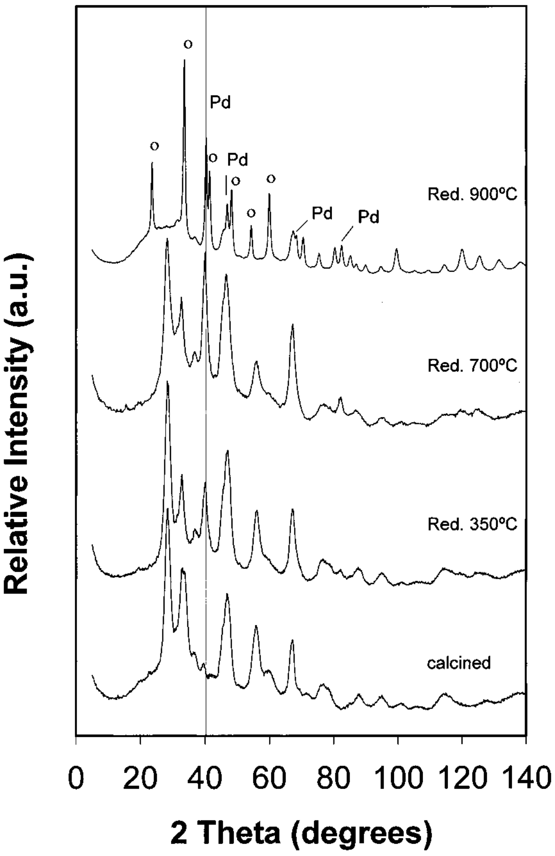

Figure 3. X-ray spectra obtained for the Pd/$Ce_{0.8}Tb_{0.2}O_{2-x}$/La_2O_3–Al_2O_3 catalyst reduced at various (indicated) temperatures and calcined in air at 500 °C for 2 h. Peaks characteristic of the aluminate phase ($LnAlO_3$) are labeled O.

When the reduction temperature increases to 700 °C, the corresponding diffractogram retains essentially the same features as those observed after reduction at 350 °C. In good agreement with previous observations made on the sample without the metal component,[7] the presence of peaks characteristic of a fluorite-like structure suggests that the supported Ce/Tb mixed oxide is still present in the catalyst after reduction at 700 °C. Likewise, a comparison with the diagram of the catalyst reduced at 350 °C indicates that the diffraction peaks due to Pd^0 are more intense in the sample reduced at 700 °C. Assuming that, after reduction at 350 °C, the metal is already completely reduced, this observation suggests that some sintering of the metal takes place as T_{redn} is increased to 700 °C. Thus, very small palladium particles present in the catalyst reduced at 350 °C that are not detectable by XRD might have been incorporated into larger ones, thus increasing the mass of microcrystals responsible for the (111) Pd peak and, consequently, the percentage of metal detectable by the technique.

Finally, structural changes induced by the most severe reduction treatment at 900 °C are more drastic. As shown in Figure 3, the XRD profile obtained after this treatment no longer exhibits the peaks characteristic of the fluorite structure of the Ce/Tb mixed oxide. Instead, a set of new diffraction lines at positions close to those reported for a perovskite-like $LnAlO_3$ phase is observed.[7] This aluminate phase must be formed by the reaction of the alumina support with the Ln^{3+} ions, either La^{3+} or the Ce^{3+} and Tb^{3+} resulting from the reduction of the supported Ce/Tb mixed oxide. Additionally, the peaks characteristic of metallic palladium have become even narrower, denoting further sintering of the metal.

3.2. HREM. Figure 4 shows two HREM images representative of the structure of the catalyst after reduction at 350 °C. Palladium is present as small fcc metallic particles that are only a few nanometers in dimension. In particular, the image in Figure 4a shows

---

(16) McCarty, J. G. *Catal. Today* **1995**, *26*, 283.

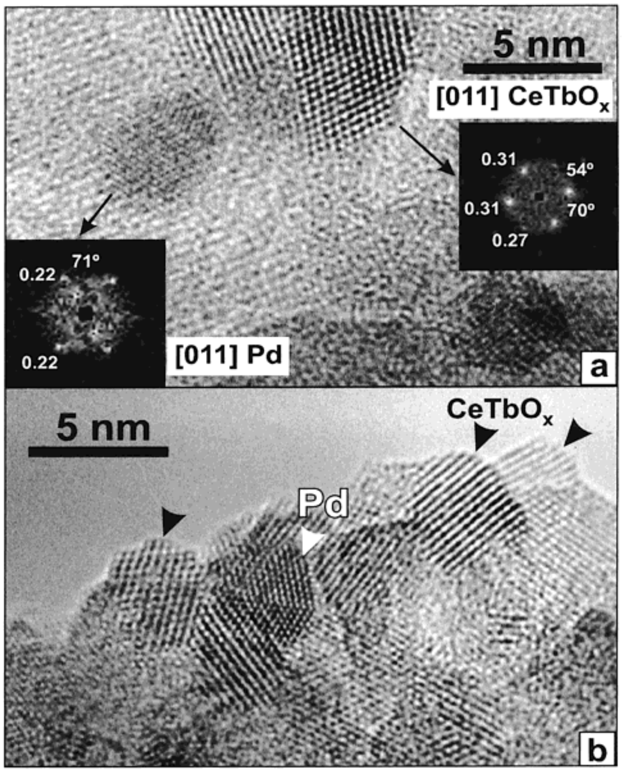

Figure 4. Experimental HREM micrographs representative of the Pd/$Ce_{0.8}Tb_{0.2}O_{2-x}$/La_2O_3−Al_2O_3 catalyst after reduction at 350 °C. The DDP insets in a were calculated from the regions indicated by arrows.

a 3-nm Pd particle close to a $\langle 110 \rangle$-type zone axis. Thus, the DDP inset at the left shows 0.22-nm spots and an interplanar angle of 71°, characteristic of {111} Pd lattice planes. The mixed oxide component is also present as nanometer-sized particles. In Figure 4a, a patch of $Ce_{0.8}Tb_{0.2}O_{2-x}$ is observed close to the metal particle. The 0.31- and 0.27-nm lattice spacings characteristic of the fluorite-type structure of this oxide can be readily measured in this region of the image. Figure 4b allows a better appreciation of the size and dispersion of these mixed oxide particles. In this image, several $Ce_{0.8}Tb_{0.2}O_{2-x}$ crystals about 5 nm in size are observed in orientations close to [110] (marked with black arrows).

The palladium and mixed oxide nanocrystals in general are evenly distributed over the surface of the La-doped alumina support. Although in some cases, such as that depicted in Figure 4b, Pd grows on the surface of the mixed oxide particles, this phenomenon is atypical as these two components are mostly found isolated on the alumina support.

Similar structural features have been observed for $T_{\mathrm{redn}} = 700$ °C (Figure 5). In this case, only a slight sintering of the Pd and of the mixed oxide takes place. In fact, the average particle size of Pd increases from 1.9 nm at 350 °C to 2.4 nm at 700 °C, whereas the average diameter of the mixed oxide particles changes from 6.5 to 7.8 nm.

When the temperature of reduction is increased to 900 °C, drastic structural changes occur. In particular, severe sintering of the Pd particles takes place. As depicted in Figure 6, after this treatment, fcc-type Pd particles with diameters of about 20 nm (i.e., 8 times the average value found at 700 °C) are observed. By measuring the average spacing of {111} Pd planes on intensity profiles of particles such as that shown in Figure 6, which exhibits a large number of these planes, a value of 0.223 ± 0.001 nm was determined. This value, which corresponds very closely to that of bulk Pd, indicates that no discernible expansion of the metal lattice takes place after reduction at high temperature. In the case of Pd/CeO_2 catalysts, Kepinski et al.[17] deduced, from an analysis of XRD and HREM data, the occurrence of Pd lattice expansion after reduction at 800 °C resulting from the incorporation of cerium into the metal lattice. Such a phenomenon does not seem to take place in our Pd/$Ce_{0.8}Tb_{0.2}O_{2-x}$/La_2O_3−Al_2O_3 catalyst system.

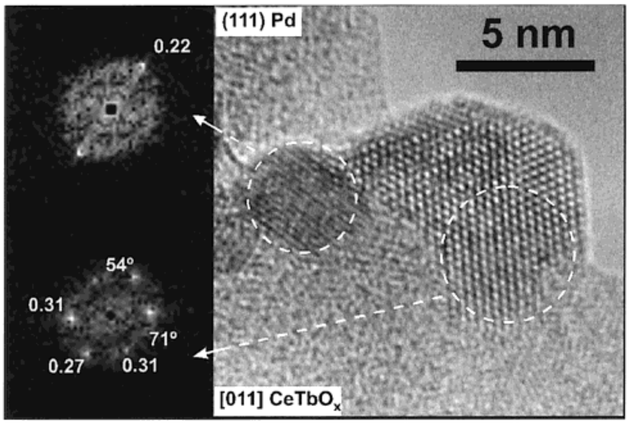

Figure 5. HREM micrograph recorded for the Pd/$Ce_{0.8}Tb_{0.2}O_{2-x}$/La_2O_3−Al_2O_3 catalyst reduced at 700 °C.

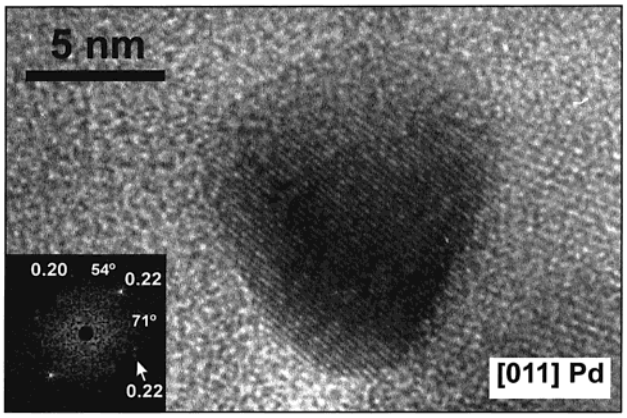

Figure 6. HREM micrograph recorded for the Pd/$Ce_{0.8}Tb_{0.2}O_{2-x}$/La_2O_3−Al_2O_3 catalyst reduced at 900 °C. A sintered Pd particle is observed.

In contrast to Pd, the structure of the mixed oxide particles after reduction at 900 °C is dramatically modified. The high-temperature treatment under reducing conditions promotes the reaction of the La-modified alumina support with the reduced mixed oxide crystallites, which are, in fact, transformed into perovskite phases ($LnAlO_3$). These latter phases have been identified from HREM images, such as those shown in Figure 7.

Several different zone axis orientations of the $LnAlO_3$ phase have been observed. In Figure 7a, a small crystal along [011] has been detected. In Figure 7b, a large

---

[17] Kepinski, L.; Wolcyrz, M. *Appl. Catal. A: Gen.* **1997**, *150*, 197.

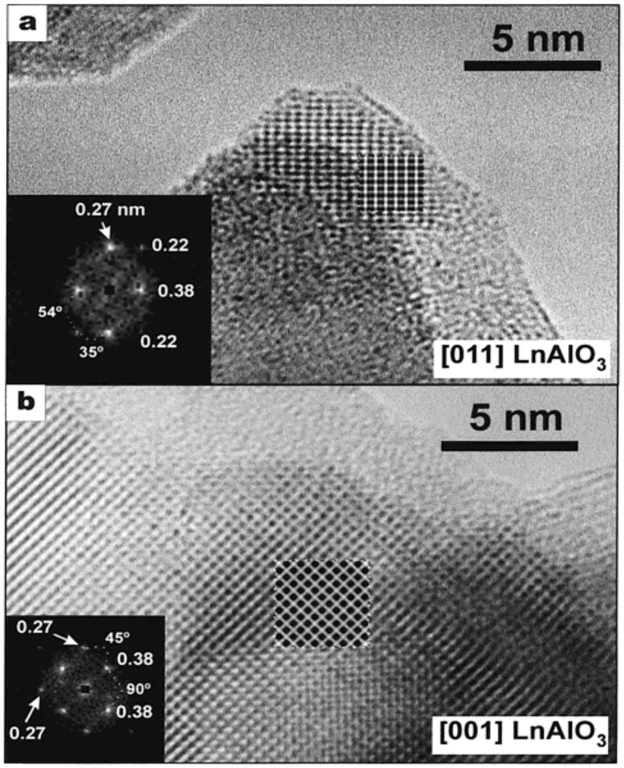

Figure 7. HREM micrographs of aluminate phases in the Pd/$Ce_{0.8}Tb_{0.2}O_{2-x}$/La_2O_3−Al_2O_3 catalyst reduced at 900 °C. The [011] and [001] projections of lanthanide aluminate phases are shown.

aluminate area along [001] has been imaged. These assignments have been confirmed by simulation (insets within dashed lines in the HREM images). Note the close match between the fringe contrasts exhibited by the experimental and calculated images.

3.3. Energy Dispersive X-ray Analysis (EDS). Additional analysis of the catalyst reduced at 900 °C by EDS has revealed complementary information about the relative proportions of lanthanide elements in the perovskite crystallites. Figure 8 shows EDS spectra representative of the two oxide support compositions commonly found in this heavily reduced catalyst. Note that, in both cases, peaks characteristic of the three lanthanide elements (La, Ce, and Tb) are present in the spectra, albeit with different proportions, as well as those due to the Al present in the perovskite.

The spectrum shown in the upper part of Figure 8 was recorded on a small perovskite particle, such as that shown in Figure 7a. In this case, the peaks due to Ce are more intense than those coming from La. This would suggest that these small aluminate particles are Ce/Tb rich. In contrast to this result, the spectrum presented in the lower part of Figure 8, which was recorded from extended aluminate regions such as those imaged in Figure 7b, is dominated by the contribution of La peaks.

In summary, the EDS results confirm, from direct compositional measurements, the formation of the aluminate phase. Moreover, the EDS spectra suggest that two types of aluminate phases are formed after reduction at high temperature (900 °C): a La-rich aluminate phase, in the form of extended regions over the surface of alumina, and a Ce/Tb rich phase in the form of small 3D supported particles.

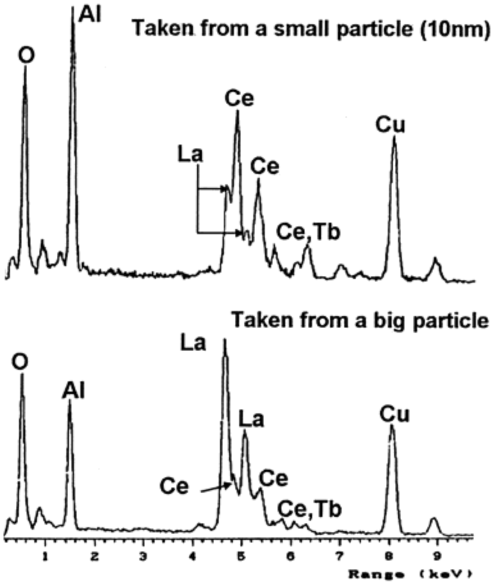

Figure 8. EDS spectra recorded for the Pd/$Ce_{0.8}Tb_{0.2}O_{2-x}$/La_2O_3−Al_2O_3 catalyst reduced at 900 °C. Representative spectra from small and large lanthanide aluminate particles are shown.

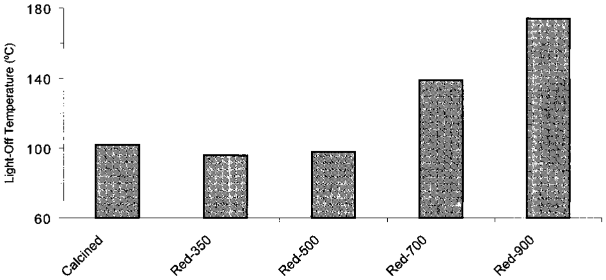

Figure 9. Light-off temperatures in the CO oxidation reaction obtained for the Pd/$Ce_{0.8}Tb_{0.2}O_{2-x}$/La_2O_3−Al_2O_3 catalyst calcined in air at 500 °C and reduced at the temperatures indicated.

3.4. CO Oxidation. As indicated in the Introduction, the behavior of the Pd/$Ce_{0.8}Tb_{0.2}O_{2-x}$/La_2O_3−Al_2O_3 catalyst for the CO oxidation reaction was also studied. This investigation was performed in an attempt to investigate the impact of the observed nanostructural changes on the catalytic behavior in a reaction of particular relevance to the TWC process.

Figure 9 is a plot of the light-off temperature values determined from running the reaction after each indicated thermal treatment. According to these data, reduction treatments at 350 and 500 °C lead to catalysts with similar activities. This result is in good agreement with our structural characterization experiments, which suggested that, up to 500 °C, both palladium and the Ce/Tb mixed oxide remain well dispersed.

After reduction at higher temperatures, 700 or 900 °C, a significant increase in the light-off temperatures is observed. This decay in the activity values correlates quite well with modifications observed in the nanostructure, namely, the sintering of the Pd and the Ce/Tb mixed oxide and the formation of the aluminate. Stabilization of Ce^{3+} and Tb^{3+} ions in the matrix of this aluminate phase could contribute to the blocking of the redox properties of the mixed oxide and possibly, in this way, counteract the promotional effect of this phase in the CO oxidation reaction.

4. Conclusions

In this work, the nanostructural changes undergone by a $Pd/Ce_{0.8}Tb_{0.2}O_{2-x}/La_2O_3-Al_2O_3$ catalyst after reduction at increasing temperatures in the range 350−900 °C have been determined. The results obtained by an array of complementary techniques including XRD, HREM, and EDS are in good agreement. A parallel study of the catalytic activity of the sample for the CO oxidation reaction has been carried out. The main conclusions from this investigation can be summarized as follows:

(1) After calcination in air at 500 °C, i.e., a thermal treatment in which the sample is not yet reduced, Pd is fully oxidized in the form of PdO and Pd_7O_8 particles. The Ce/Tb mixed oxide is also present as nanocrystals. The reaction of these cerium/terbium oxide crystallites with the lanthana-modified alumina is negligible.

(2) The treatment with H_2 (5%)/Ar at 350 °C leads to reduction of palladium, which now transforms into nanosized metallic particles. A subtle increase in activity with respect that of the oxidized catalyst is also observed. The Ce/Tb promoter is still present and well-dispersed as oxide nanoparticles.

(3) Increasing T_{redn} in the range 350 °C−700 °C gives rise to sintering of both Pd and the Ce/Tb mixed oxide particles.

(4) Upon reduction at 900 °C, Pd sinters severely, and at the same time, the extensive formation of a perovskite-like $LnAlO_3$ phase takes place. Moreover, according to EDS measurements, two distinct aluminate phases are in fact formed: one Ce/Tb-rich and the other La-rich.

(5) The nanostructural modification observed in the 700−900 °C T_{redn} range can be correlated with a steep decrease in the catalytic activity of the system for the CO oxidation reaction.

Acknowledgment. This work received financial support from CICYT (Project MAT99-0570) and the “Junta de Andalucía”. XRD diffractograms as well as HREM images were obtained at the Science and Technology central facilities of UCA. EDS spectra were acquired at the Department of Materials Science and Engineering, University of Liverpool.

CM011260Y